FISEVIER

Contents lists available at ScienceDirect

Applied Geochemistry

journal homepage: www.elsevier.com/locate/apgeochem



Radium attenuation and mobilization in stream sediments following oil and gas wastewater disposal in western Pennsylvania



Katherine Van Sice^a, Charles A. Cravotta III^b, Bonnie McDevitt^a, Travis L. Tasker^a, Joshua D. Landis^c, Johnna Puhr^a, Nathaniel R. Warner^{a,*}

- ^a Civil and Environmental Engineering Department, The Pennsylvania State University, University Park, PA, 16802, USA
- ^b U.S. Geological Survey, Pennsylvania Water Science Center, 215 Limekiln Road, New Cumberland, PA, 17070, USA
- ^c Department of Earth Sciences, Dartmouth College, 6105 Fairchild Hall, Hanover, NH, 03755, USA

ARTICLE INFO

Editorial handling by Dr D A. Kulik

Keywords:
Barite
Celestite
Brine
Adsorption
Manganese & iron oxides
Precipitation

ABSTRACT

Centralized waste treatment facilities (CWTs) in Pennsylvania discharged wastewater from conventional and unconventional oil and gas (O&G) wells into surface waters until 2011, when a voluntary request from the Pennsylvania Department of Environmental Protection (PA DEP) encouraged recycling rather than treating and discharging unconventional O&G wastewater. To determine the effect of this request on the occurrence of radium in streams, we sampled sediments at five CWTs that processed conventional O&G wastewater from 2011 to 2017 and compared results to published data. Despite the policy change in 2011 that reduced disposal of unconventional wastes (i.e., Marcellus) to surface water in Pennsylvania, the continued disposal of conventional O&G wastewater led to elevated radium activities in sediments at the point of discharge that were often hundreds of times higher than background. While these elevated activities were also present in downstream sediments (1.5 × higher than background), the elimination of unconventional O&G wastewater disposal through the CWTs since 2011 decreased radium loading to the stream by approximately 95%.

Sequential extractions and geochemical modeling using PHREEQC indicate that radium likely co-precipitates with barite or barite-celestite solid solutions and accumulates in the sediment as treated O&G effluent enters the stream. Adsorption of "exchangeable" radium, barium, and strontium on hydrous iron and manganese oxide coatings on fine-grained stream sediments is an important radium sequestration mechanism further downstream that can decrease the cation concentrations and potential for radio-barite co-precipitation. Radium downstream of CWTs was more abundant and more available for dissolution and desorption than radium in upstream sediments.

1. Introduction

Oil and gas (O&G) production in Pennsylvania generates billions of liters of wastewater per year that has high concentrations of total dissolved solids (TDS), heavy metals, and naturally occurring radioactive material (NORM) (Dresel and Rose, 2010; Kargbo et al., 2010; Osborn and McIntosh, 2010; Rowan et al., 2011; Wilson and VanBriesen, 2012; Haluszczak et al., 2013; Akob et al., 2015; PADEP, 2016a, b). When O&G wastewater is treated in centralized wastewater treatment facilities (CWTs) and discharged to surface waters, it can impact water quality and cause elevated activities of radium in sediments (Kargbo et al., 2010; Gregory et al., 2011; Wilson and VanBriesen, 2012; Ferrar et al., 2013; Warner et al., 2013; Brantley et al., 2014; Vengosh et al., 2014; Harkness et al., 2015). Radium is a radioactive alkaline earth metal that

is found naturally throughout the environment in low activities (e.g., 78–100 Bq/kg combined radium in New York State soils) (NYDEC, 1999) but can increase cancer risks at higher concentrations, especially when ingested in drinking water (International Atomic Energy Agency, 2014). Radium-226 and radium-228 (²²⁶Ra and ²²⁸Ra), two isotopes of radium, are persistent environmental pollutants with half-lives of 1600 and 5.75 years, respectively (International Atomic Energy Agency, 2014). The US Environmental Protection Agency (USEPA) established a maximum contaminant level of 0.185 Bq/L (5 pCi/L) combined radium in public drinking water, where combined radium is defined as the sum of ²²⁶Ra and ²²⁸Ra (USEPA, 2000). Generally, radium may be expected to precipitate or sorb with other alkaline earth cations in the environment. In a freshwater aquifer and associated surface waters, radium could be in the aqueous form (primarily as Ra²⁺, and associated

E-mail address: nrw6@psu.edu (N.R. Warner).

^{*} Corresponding author.

K. Van Sice et al. Applied Geochemistry 98 (2018) 393–403

complexes, including RaOH⁺, RaCl⁺, RaCO₃0, RaSO₄0, etc.); sorbed to iron oxide (ferrihydrite, goethite), manganese oxide (manganite, todorokite, birnessite), clays (kaolinite, illite, muscovite), and organic matter; or co-precipitated with barite (BaSO₄), celestite (SrSO₄), or alkaline earth carbonates such as witherite (BaCO₃) and strontianite (SrCO₃) (Ames et al., 1983a; Langmuir and Riese, 1985[;] International Atomic Energy Agency, 2014; Sajih et al., 2014). Radium commonly coprecipitates with barite, celestite, and (Ba,Sr)SO₄ solid solutions during the O&G treatment process through the addition of sulfate (Zhang et al., 2014). The sulfate compounds, particularly barite and associated solid solutions, are relatively insoluble with a low bioaccumulation risk (Menzie et al., 2008).

Wastewaters from O&G wells in the Appalachian Basin generally are brines with higher activities of total radium compared to freshwater. However, radium activities vary depending on the origin of the O&G wastewater (Rowan et al., 2011, 2015; Blondes et al., 2017; Lauer et al., 2018). The wastewaters from unconventional O&G wells in the Appalachian Basin generally have higher radium activity (e.g., 91 Bq/L for Marcellus Shale) than wastewaters from conventional gas formations (median = 27 Bq/L) (Rowan et al., 2011, 2015). Unconventional reservoirs also have higher parent ²³⁸U/²³²Th ratios than conventional formations resulting in lower ²²⁸Ra/²²⁶Ra ratios (median value of 0.19) in unconventional wastewater compared to conventional wastewater (median value of 1.04) (USEPA, 2011; Warner et al., 2013; Hladik et al., 2014; Harkness et al., 2015; PADEP, 2016a, b; Lauer et al., 2018) or typical groundwater from sandstone aquifers (Vengosh et al., 2009; Szabo et al., 2012). Thus, ²²⁸Ra/²²⁶Ra ratios are useful for distinguishing conventional and unconventional wastewaters (Rowan et al., 2011, 2015) which are otherwise similar in terms of major element chemistry (Chapman et al., 2013; Haluszczak et al., 2013). The ratios have been used to help determine the sources of contamination in both accidental spills and at disposal sites (Hladik et al., 2014; Akob et al., 2016; Cozzarelli et al., 2017; Lauer et al., 2018).

In Pennsylvania, prior to 2011, publicly owned treatment works (POTWs) for domestic sewage and CWTs were permitted through the National Pollutant Discharge Elimination System (NPDES) and accepted and unconventional O&G conventional Unconventional O&G wastewater discharged through NPDES permitted facilities peaked in 2009 and decreased thereafter, following reports of elevated concentrations of bromide and associated organohalide compounds in source water intakes downstream of treatment facilities in western Pennsylvania (Hladik et al., 2014; Good and VanBriesen, 2016). In April 2011, the Pennsylvania Department of Environmental Protection (PA DEP) requested that O&G producers stop disposing produced water from unconventional shale development at wastewater treatment facilities with NPDES permits (Ferrar et al., 2013; Good and VanBriesen, 2016). Operators largely complied with this request and, as a result, O&G wastewater discharge to surface water decreased by 50% from 2011 to 2014 while the use of recycled O&G wastewater for hydraulic fracturing dramatically increased (Burgos et al., 2017). Despite these changes in the management of unconventional wastewaters, conventional wastewater continues to be accepted at CWTs and discharged to surface water through NPDES permits.

Although O&G wastewaters are treated at NPDES permitted facilities, concentrations of radium are generally found to be elevated in downstream river sediments (Warner et al., 2013; PADEP, 2016a, b; Burgos et al., 2017; Lauer et al., 2018). In 2011, 2012, sediments at a CWT effluent discharge in Blacklick, PA contained radium activities 200 times greater than concentrations upstream; however, that study only investigated one facility and did not collect samples more than 1800 m downstream of the discharge (Warner et al., 2013). Sediment samples collected near the discharges of multiple CWT facilities after 2011 have higher ²²⁸Ra/²²⁶Ra ratios than earlier samples, which indicate that conventional O&G wastewater discharged from 2011 to 2017 contributed to radium accumulation in sediments (Lauer et al., 2018). Sediments would be expected to contain the lower ²²⁸Ra/²²⁶Ra

ratios if the elevated residual radium was from past disposal practices containing conventional O&G wastewater (Lauer et al., 2018). Two studies conducted by PA DEP contractors also reported elevated radium activity in sediments collected from discharge points at three CWT sites in 2010, 2013, and 2014 (USEPA, 2011; PADEP, 2016a, b). Additionally, in 2015, researchers observed radium activities 3 to 4 times background activities in a sediment core from the Conemaugh River Lake, 19 km downstream of a CWT that treated unconventional wastewater (Burgos et al., 2017). Other investigations of sediments collected from discharge points of five POTWs in western Pennsylvania that accepted O&G wastewater did not document radium significantly elevated from background concentrations (Skalak et al., 2014). Although previous studies have demonstrated increased radium activity at the point of CWT discharges, no study has evaluated the distribution (a) at a larger spatial scale (b) the temporal nature of the changes downstream and (c) the mineralogy and ultimate mobility of the radium in the sediments.

The goals of this project were: (1) to characterize radium activities and distribution over an extended 58 km transect upstream and downstream of O&G wastewater treatment facilities for evidence of watershed-scale impacts, (2) to assess if the 2011 request from the PA DEP to recycle unconventional O&G wastewater rather than dispose it at CWTs resulted in decreased radium activities in sediments at the points of discharge, and (3) to determine the solid-phase associations and potential mobility of radium in the sediment upstream and downstream of the treatment facilities.

2. Materials and methods

2.1. Sample Collection

We collected grab sediment samples from the upper 5 cm of the sediment surface upstream, downstream, and at the point of discharge from five NPDES- permitted O&G wastewater discharges in western Pennsylvania that discharge to Blacklick Creek (CWT-A and -B), the Conemaugh River (CWT-C), and the Allegheny River (CWT-D and -E). All the facilities, excluding CWT-B, reported accepting unconventional O&G wastewater from 2007 to 2011. CWT-B reported accepting only conventional O&G wastewater. The sediment sampling avoided large boulders or gravel that were present at some facilities. Sediment samples near the point of discharge were collected in duplicate during multiple sampling events from 2011 to 2017 at locations within 1-5 m of the discharge pipe depending on both water flow conditions and the presence of boulders. Separately, the Blacklick Creek transect (58 km) consisted of samples (total n = 80) collected in August 2016 (n = 40), December 2016 (n = 8), or July 2017 (n = 32) (Fig. 1). These samples were collected from the right bank of the stream every kilometer $(\pm 100 \,\mathrm{m})$ along the transect. Samples were typically collected in 1-10 cm water depth.

2.2. Radium Measurement

Sediment samples were dried in an oven at 60 °C, ground to homogeneity using a mortar and pestle, and sieved through a 1.18 mm sieve. Samples were then packed into 20 mL high-density polyethylene scintillation vials. Prior to measurement, vials were sealed and taped for a minimum of 20 days to allow $^{226}\mathrm{Ra}$ daughter decay products ($^{222}\mathrm{Rn}$, $^{214}\mathrm{Pb}$, and $^{214}\mathrm{Bi}$) to reach secular equilibrium (Parekh et al., 2003). For CWT effluent samples, radium was extracted by BaSO₄ precipitation, collected on filter paper and then measured. For sediment samples collected prior to 2016, $^{226}\mathrm{Ra}$ and $^{228}\mathrm{Ra}$ were measured on an ultra-low background broad energy germanium (BEG) detector manufactured by Canberra Instruments located at Dartmouth College Short-Lived Radionuclide Laboratory in Hanover, NH.

For sediment samples collected after 2016, radium was measured with a small anode germanium detector (SAGe) manufactured by

K. Van Sice et al. Applied Geochemistry 98 (2018) 393–403

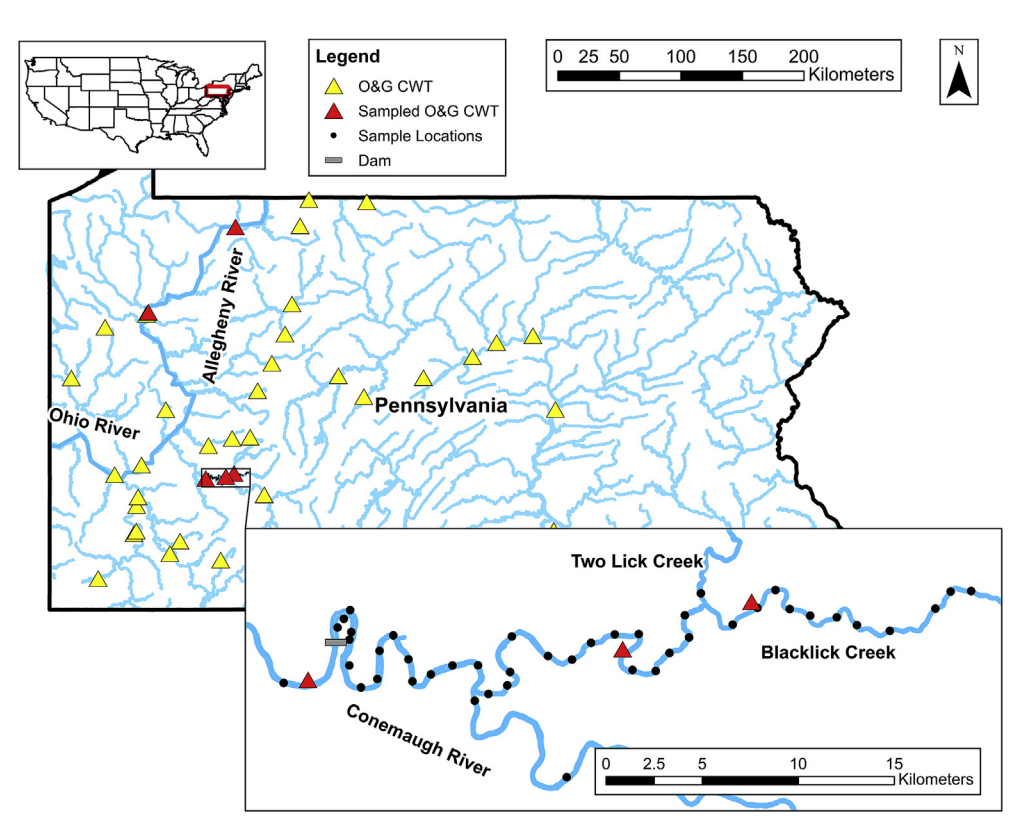


Fig. 1. Location of CWTs and POTWs that accepted O&G wastewater (yellow triangles) in Pennsylvania. Five CWTs were sampled during this study (red triangles), including a detailed transect that collected 80 sediment samples over roughly 58 km of stream length that included locations both above and below three CWTs (A, B and C). CWT is centralized waste treatment facility; POTWs is publicly-owned treatment works. (For interpretation of the references to colour in this figure legend, the reader is referred to the Web version of this article.)

Canberra Instruments located at Penn State University's Tracing Salinity with Isotopes (SALTS) lab. Additional details regarding radium measurement methods are in the Supplemental Information section. All samples were measured in the same vessel geometry as the calibration standards uranium ore tailings (UTS-2, UTS-3, and UTS-4) obtained from Canadian Certified Reference Material Project through Natural Resources Canada with certified ²²⁶Ra and ²²⁸Ra activities of 5.6 Bq/g and 1.0 Bq/g, respectively. The UTS standards had a similar density (1.47 g/mL) compared to prepared samples (1.1–1.47 g/mL). Samples were measured until counting uncertainty errors were less than 5% for each energy, typically between 6 and 24 h.

2.3. Sediment Characterization

The grain size distribution of a subset of dry sediment samples post-pulverization was measured by sieving and measuring the mass that passed through each sieve. Sediments were sieved into three sizes: coarse sands ($>300\,\mu\text{m}$), fine sands (300–45 μm), and silts and clays ($<45\,\mu\text{m}$). The mineralogy of the sediments was analyzed by quantitative X-ray diffraction (XRD) using a X'Pert PRO MPD located in the Materials Characterization Lab at The Pennsylvania State University and Jade software. Scanning Electron Microscopy (SEM) and Energy Dispersive X-ray Spectroscopy (EDS) were done using a FEI Quanta 200 Environmental SEM and Aztec software.

Radium distribution in selected sediment samples (n = 4) from upstream, at the point of discharge of CWT-A, and downstream of CWT-B was determined with a four-step sequential-extraction procedure (Stewart et al., 2015; Tasker et al., 2016). The procedure was performed in duplicate and targeted (1) soluble salts using ultrapure water; (2) surface exchangeable and low-charge interlayer cations using ammonium acetate buffered to pH 8; (3) carbonate minerals using 8% acetic acid; and (4) high-charge interlayer cations, partial silicates, and oxides using 0.1 M hydrochloric acid. The aqueous solutions were added to sediments at a 20:1 vol:mass ratio. The first extraction was shaken for 24 h and the second, third, and fourth were shaken for 12 h. Selected extracts were analyzed for major cations and trace metals (see

supplemental material). Following each leaching step, the solid residue was rinsed and centrifuged 3 times with ultrapure water. Then, the sediments were freeze dried and the radium activity was measured before proceeding to the next extraction step.

Radium sorption experiments were conducted on a subset of dry sediments collected upstream of CWT-A and CWT-E. Sediments were sieved to less than 1.18 mm and then mixed with a brine collected from a conventional gas well containing 115 \pm 4 Bq/L 226 Ra and 27 \pm 1 Bq/L 228 Ra. The sediment (20 g) was mixed with 200 mL of diluted brine (50×, 25×, and 5× dilution) for 24 h on a shaker table. The sediments were rinsed three times with distilled water following the application of the diluted brine and then freeze dried. Radium activity in the dried sediments was measured prior to and after brine application to determine radium sorption.

2.4. Statistical Analysis

The statistical program R (version 3.1.2) was used to conduct Kruskal- Wallis tests, regressions, and pairwise Wilcoxon rank sum tests with Bonferroni corrections for multiple comparisons. Values to the fourth decimal point were used to conduct Wilcoxon rank sum tests. The Blacklick Creek and Conemaugh River streambed sediment data from sampling in 2016 and 2017 was combined and then divided into three sections: upstream of all CWTs (U, n = 18), downstream of CWT-A (A, n = 12), and downstream of CWT-B (B, n = 46). The point of discharge at CWT-A was omitted from these sections to prevent the high radium activity value from skewing the mean for the downstream segments. The point of discharge of CWT-B was not readily accessible, but we estimate the nearest sample point to the discharge pipe to be approximately 1 km downstream.

2.5. Geochemical Modeling Methods

The aqueous geochemical program, PHREEQC (Parkhurst and Appelo, 2013), was used to compute aqueous and surface speciation and potential for selected minerals to precipitate as pure phases or solid

solutions from the median CWT-A effluent and associated upstream and downstream waters. To evaluate the attenuation of radium by dilution and chemical interactions after discharge of the effluent, samples representing the point of discharge at CWT-A and the upstream water of Blacklick Creek were mixed in various proportions (up to 10% CWT-A by volume), consistent with the relative flow volumes of the river and NPDES discharge during high-to low-flow conditions (Table S8). Four different scenarios were simulated, all with the same range of mixing fractions (Table S9) and initial water chemistry (Table S10): (1) conservative mixing, (2) mixing plus precipitation of pure mineral phases, (3) mixing plus precipitation of pure and solid-solution phases, and (4) mixing, mineral precipitation, and adsorption of radium, barium, strontium, and other ions by hydrous ferric oxide (HFO) and hydrous manganese oxide (HMO). The potential for co-precipitation of radium with barium was evaluated assuming ideal, binary (Ba,Ra)SO4 solid solution of barite and RaSO₄. Thermodynamic data from "wateq4f.dat" (Ball and Nordstrom, 1991) were supplemented with additional data for radium species and phases from Langmuir and Riese (1985) and "sit.dat" (Giffaut et al., 2014) provided with PHREEQC. Sorption of cations and anions on HFO considered the monoprotic, diffuse double layer (MDDL) model of Dzombak and Morel, (1990) with surface binding coefficients for radium and barium reported by Sajih et al. (2014). Sorption of cations including barium and strontium on HMO considered the MDDL model of Tonkin et al. (2004). The binding coefficient for radium on HMO was estimated using its first hydrolysis constant and linear free energy relation (LFER) reported by Pourret and Davranche (2013) based on the data of Tonkin et al. (2004).

A second set of PHREEQC models simulating the adsorption of radium, barium, and strontium by HFO and HMO was developed to demonstrate potential interactions (competition) between the formation of (Ba,Ra)SO₄ solid-solution and adsorption of Ra, Ba, and Sr as a function of pH, solute concentrations, and sorbent mass and composition. Two solution concentrations were considered based on previous simulated mixtures of CWT-A and Blacklick Creek (1) 1% CWT-A and (2) 10% CWT-A. Either HFO or HMO was specified as the sorbent surface for a range of different masses per liter of solution: 0.010 g-1.0 g. Adsorption simulations included precipitation of (Ba,Ra) SO₄ solid solution. The four modeled scenarios demonstrate (1) potential for elevated radium in solution, absent precipitation or adsorption reactions, (2) potential for pure phases to limit barium, strontium, and radium concentrations; (3) potential for solid solutions to limit barium and radium concentrations, and (4) interplay between precipitation and adsorption as possible controlling processes of barium, strontium, and radium. Example PHREEQC codes used for both sets of simulations and selected graphical results are included with Supplemental Information.

3. Results and discussion

3.1. Temporal Radium Activities in Sediments

Despite the decrease in discharge of unconventional O&G wastewater from treatment facilities to streams, radium activity in sediments at the point of discharge at three treatment facilities remained elevated after 2011 (Fig. 2 and Fig 3). Sediments near the point of discharge at CWT-A and CWT-D had the highest total radium activities in 2014 with $15,000 \pm 200 \, \text{Bg/kg}$ and $24,600 \pm 740 \, \text{Bg/kg}$, respectively (Fig. 2).

In 2015, CWT-A underwent remediation where sediments were removed from the streambed at the point of discharge for roughly 10 m into the stream and 200 m downstream (Fig. S1). Prior to remediation, the radium activity at CWT-A was greater than 7400 Bq/kg (Fig. 2) with 228 Ra/ 226 Ra ratios from 0.22 to 0.47. Following remediation, sediments collected at the point of discharge of CWT-A in 2016 contained radium activity of 407 \pm 15 Bq/kg and then in 2017 sediments contained 1591 \pm 22 Bq/kg. Although the remediation was effective in reducing radium concentrations at CWT-A, the subsequent increase in radium at

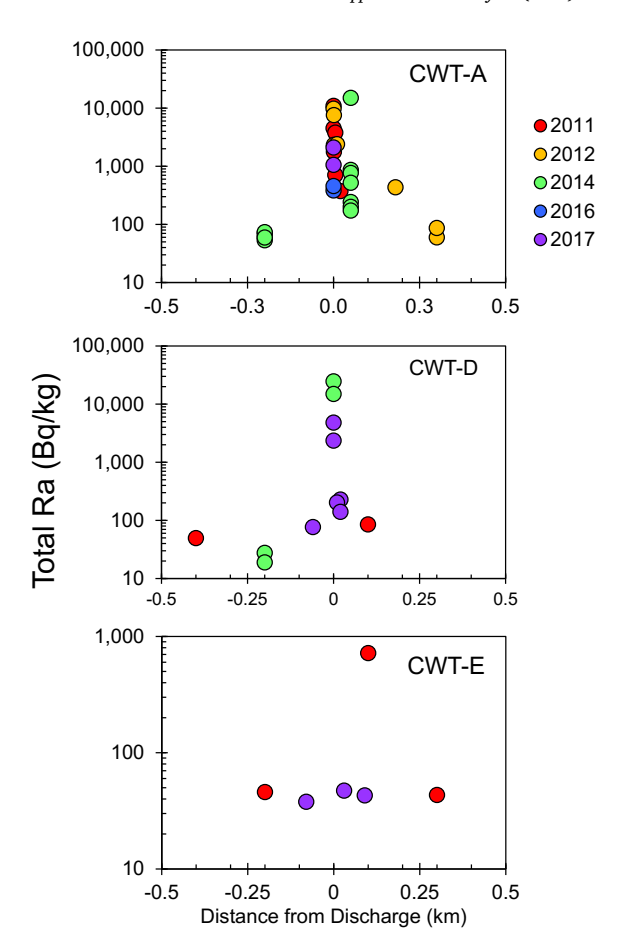


Fig. 2. Total radium (228 Ra + 226 Ra) in surficial sediments collected at three CWT locations (A, D, and E) as shown on Fig. 1. A negative distance from discharge indicates distance upstream whereas a positive distance indicates distance downstream from the discharge.

the discharge suggests that the stream may require remediation again in the future since radium activities are above the USEPA limits of 5 pCi/g (185 Bq/kg) above background. At the point of discharge of CWT-A, the $^{228}\mbox{Ra}/^{226}\mbox{Ra}$ ratios in sediments increased from 0.58 in 2016 to 0.82 in 2017, suggesting conventional O&G wastewaters with higher $^{228}\mbox{Ra}/^{226}\mbox{Ra}$ were the source.

Compared to the other facilities, CWT-E had low radium accumulation with 48 ± 4 Bq/kg being the highest radium concentrations measured in 2017. These low measurements could result from various factors such as low activities in the effluent at the facility because of better treatment or variability over time in the treatment performance for removing metals as observed previously (Ferrar et al., 2013). It is important to note that another previous study found higher activity at the point of discharge for CWT-E (Lauer et al., 2018), indicating there is large variability in radium activity at small temporal or spatial scales.

The radium activity at CWT-D decreased in 2017 but was 4810 ± 111 Bq/kg which is well above regulations that designate 185 Bq/kg above background as a standard for land surfaces impacted by radioactive waste materials (40 CFR §Section 192.12) or materials that can be landfilled [(ORC § 3734.02 (P)(2)]. Overall, the results demonstrate that both conventional and unconventional wastewater increased radium activities in sediments at three CWTs (Fig 2 and Fig. 3). Despite the apparent increase in radium at CWT-A following 2011, our estimates suggest that activities would have been much higher if facilities had continued to accept unconventional O&G wastewater.

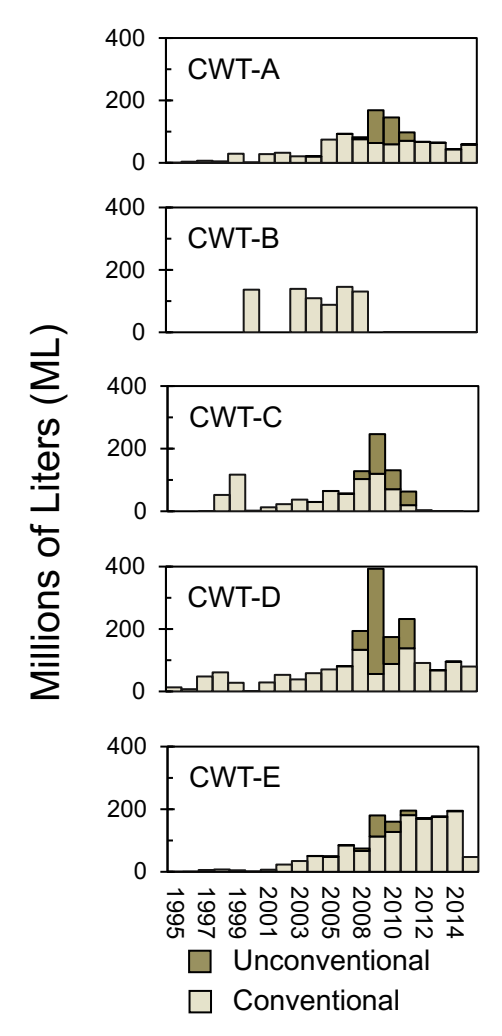


Fig. 3. Volumes in million liters (ML) of O&G wastewater accepted from 1995 to 2015 at five CWT locations (A-E, Fig. 1). Unconventional O&G wastewater accepted at treatment facilities decreased following 2011.

3.2. Wastewater and Surface Water Characterization

We estimated the 226 Ra loads from CWT-A and -D during 2011–2015 using effluent radium activities reported by the USEPA (USEPA, 2011) and disposal data reported on the PADEP O&G reporting website for two scenarios: (1) the actual discharge and (2) the discharge if facilities had continued to accept unconventional wastewater. The volumes of unconventional and conventional O&G wastewater accepted at five CWTs, including CWT-A and CWT-D, from 1995 to 2015 are shown in Fig. 3. We assumed the discharge volumes for scenario 2 were the mean of the volumes during the time CWTs were accepting unconventional O&G wastewater (2008–2011). Based on these assumptions, CWT-A and CWT-D would have discharged $\sim 80\%$ and $\sim 120\%$ more O&G wastewater without the voluntary request from the PA DEP.

Due to the uncertainty in predicting discharge volumes from the CWTs and effluent radium concentrations over time, we acknowledge that there are uncertainties in radium load estimates from the CWTs. For CWT-A, the mean 226 Ra activities were 2 Bq/L (n = 2) prior to 2011 and 0.1 Bq/L (n = 12) during 2011–2015. The activities modeled for CWT-D were 4 Bq/L (n = 2) before and 0.3 Bq/L (n = 1) after the facility stopped accepting unconventional wastewater. The data suggest that the elimination of unconventional O&G wastewater after 2011 may have reduced 226 Ra loads by \sim 95% of the pre-2011 load. Due to high standard deviation in reported effluent activities and NPDES reported discharge volumes, calculated reductions are imprecise but suggest the

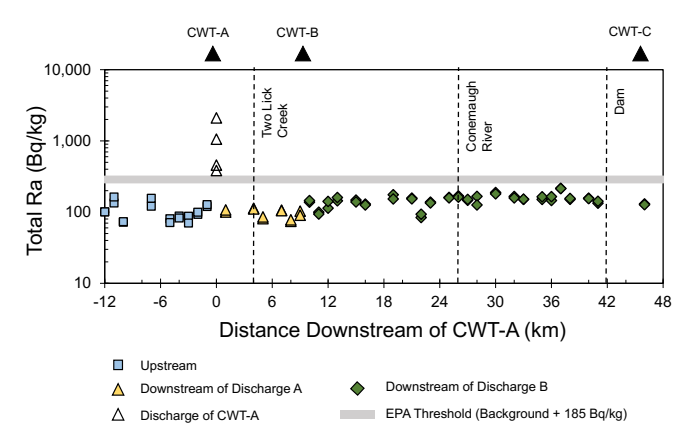


Fig. 4. Radium activities (228 Ra + 226 Ra) in sediments collected in 2016–2017 along a \sim 58 km transect that stretched upstream and downstream of three CWTs. For statistical analyses, the transect was divided into three sections: upstream (U), downstream of CWT-A (A), and downstream of CTW-B (B).

2011 policy change resulted in notable decreases in the volume of unconventional O&G wastewater and associated radium discharges to streams.

3.3. Spatial Distribution of Radium in River Sediments

The mean radium activity in the section upstream of CWT-A (U) was 102 ± 4 Bq/kg which is consistent with reported background values in New York and Pennsylvania (NYDEC, 1999; Warner et al., 2013). At the CWT-A point of discharge, the average total radium activity of the two samples was 420 ± 14 Bq/kg (Fig. 4). Sections A and B, downstream of CWT-A and CWT-B, respectively, had mean total radium activities of 96 ± 4 Bq/kg and 149 ± 6 Bq/kg.

Section B had significantly higher mean radium activity than sections A and U (p < 0.01). Sections U and A (excluding the point of CWT-A discharge) were not significantly different. Note that these samples were collected following the 2015 remediation of CWT-A. The remediation removed sediments that were noticeably impacted and reported in 2013 (Warner et al., 2013). The mean $^{228}\text{Ra}/^{226}\text{Ra}$ ratios were 1.33 \pm 0.21 σ in section U, 0.69 \pm 0.16 σ at the point of discharge of CWT-A, 1.29 \pm 0.14 σ in section A, and 1.21 \pm 0.18 σ in section B (Table S5). The $^{228}\text{Ra}/^{226}\text{Ra}$ ratios were significantly lower (p = 0.05) in section B than U. This lower ratio in section B combined with higher activity is consistent with radium from O&G wastewater.

Radium activities in the sediments of two other background sampling locations, Two Lick Creek and upstream Conemaugh River, were lower than section B (Fig. 4) and likely did not contribute to the high radium activities observed. The elevated radium activity in section B could possibly be from a combination of CWT-A, which has a history of radium pollution (Warner et al., 2013) and CWT-B which only accepted conventional O&G wastewater. Section A was not significantly different than section U, likely due to the remediation at CWT-A that removed sediments with elevated radium. The discharge pipe of CWT-B was not observed during sampling and therefore no samples were collected directly from the point of discharge that might indicate elevated radium (or little/no radium). Therefore, the large transect of sediment indicates that O&G wastewater disposal *may* have watershed scale impacts on radium concentrations in sediments, but the overall increase is relatively small (44–52 Bq/kg).

Besides O&G wastewater discharge from the CWTs, elevated levels of radium in stream sediment could be caused by O&G brine spreading on roads, coal-mine drainage and associated sediment, ash generated from combustion processes, or physical processes that increase the amount of fine-grained materials, which preferentially sorb radium (Centeno et al., 2004; Crespo et al., 1993; International Atomic Energy Agency, 2014; Lauer et al., 2015; Burgos et al., 2017; Tasker et al.,

2016). All these mechanisms are active in the Blacklick-Conemaugh waterway and could be partially responsible for the higher radium activities observed in section B. Indiana County used O&G brine on roads for dust suppression and deicing (PADEP, 2016a, b). Though Blacklick Creek is impacted by coal mine drainage upstream of all three CWTs sampled, mine drainage is not expected to be a source of radium since measured radium activities (Warner et al., 2013) and barium and strontium concentrations (Cravotta, 2008) are very low. Additionally, abundant HFO and HMO in surficial sediments can sequester the cations from Homer City Generating Station, a coal fire plant, is located within a few miles of the sampling transect on Conemaugh River. Coal combustion residuals in the Appalachian region have a mean ²²⁸Ra/²²⁶Ra ratio of 0.67 which could contribute to the lower ratio seen in section B (Lauer et al., 2015). The Conemaugh River Dam created a low-energy zone that caused fine-grained sediments to accumulate (Burgos et al., 2017). The 31 km section of Conemaugh River where we observed elevated radium activity may be affected by O&G wastewater disposal plus additional factors, noted above, though those processes have been active far longer than the disposal of unconventional O&G wastewater and presumably stream sediment radium concentrations have already equilibrated with the other processes active for much longer duration.

3.4. Sediment Characterization and Radium Distribution

We characterized the occurrence and distribution of radium in various sediment components by particle-size separation, sequential extraction, and exposure to O&G brine (sorption experiments). The mineral and elemental components of the sediments as determined by XRD, EDS, and chemical analysis of extracts suggest that radium could be present in association with relatively inert forms, such as barite, and more labile (adsorbed) forms, such as clays (kaolinite, muscovite) or oxides (HFO, HMO).

Radium was associated primarily with fine-grained silts and clays (p < 0.01, $\rm R^2=0.76$), which have greater unit surface area than coarse sediments. The percent silt and clay composition increased with distance downstream (Fig. 5); section B had a greater fraction of silts and clays than section U (p = 0.04) or A (p = 0.01). Thus, transport and deposition of fine-grained sediment could account for the greater mean radium activities in section B compared to upstream sections.

Sediments were composed primarily of relatively inert silicates, including quartz, muscovite, and kaolinite (Fig. 6), with minor clinochlore and goethite. Muscovite, present in all samples analyzed, can

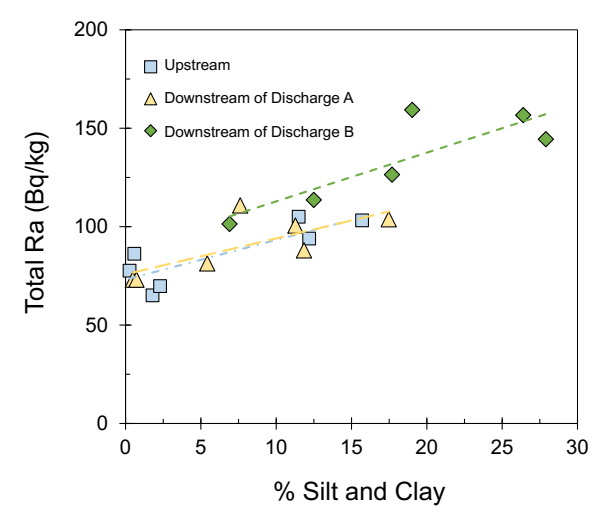


Fig. 5. (a) Radium activity (228 Ra + 226 Ra) versus % silt and clay in the sediment samples upstream (U), downstream of CWT-A (A), and downstream of CTW-B (B). Dashed lines represent regression lines.

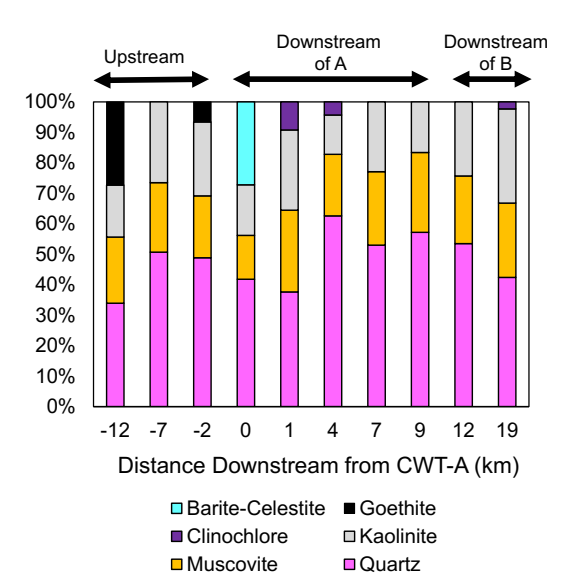
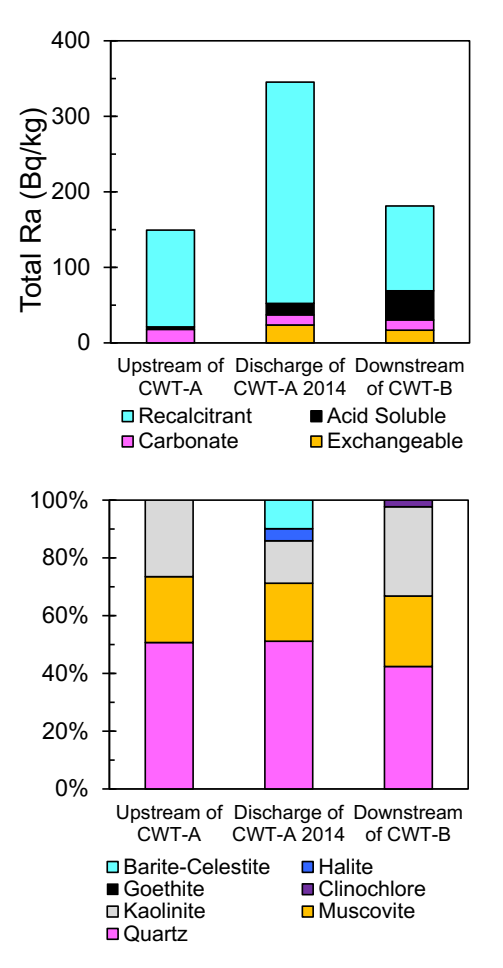


Fig. 6. Mineralogy of sediment samples collected along the Blacklick Creek and Conemaugh River Transect in 2016–2017.

sorb substantial amounts of radium and has a higher affinity for radium than kaolinite (Beneš et al., 1986). Kaolinite can rapidly sorb radium from surface waters but the bonding is weak and easily reversible (Ames et al., 1983b; Beneš et al., 1985). Quartz has a negligible impact on radium sorption (Beneš et al., 1984). Nevertheless, goethite and other HFO coatings on any of these mineral surfaces, particularly the fine-grained particles that have high unit surface area, could sorb radium and other alkaline earth cations, particularly at near-neutral pH values (Ames et al., 1983a; Dzombak and Morel, 1990; Tonkin et al., 2004; Sajih et al., 2014).

Barite, celestite, or barite-celestite solid solution ((Ba,-Sr)SO₄) were detected by XRD of sediments only at CWT-A (Fig. 7); XRD could not distinguish between the sulfate phases. No sulfate minerals were detected by XRD of sediments collected upstream or downstream of CWT-A. The EDS images of sediments collected in 2017 at the point of discharge of CWT-A indicate that barium, strontium, and sulfur frequently were co-located (Fig. S3). Barium and sulfur were also co-located in sediments collected in 2014 at CWT-A, but without strontium, which may suggest primarily barite precipitation (Fig. S2). Neither barium nor strontium was detected by EDS of sediments collected in 2016 upstream or downstream of CWT-A (Fig. S4). Further study is needed to define spatial and temporal variations in the mineral distribution and composition in the stream environment in conjunction with changes in streamflow and effluent volume and composition.

Radium in the sediment samples of our study was primarily associated with the recalcitrant solid fraction that remained after the completion of four progressively more aggressive leaching steps (Fig. 7). The percentage of recalcitrant radium was 86% for upstream sediments, 85% for sediments at CWT-A discharge, and 62% in section B sediments. The recalcitrant radium could be associated with barite; barite would not be dissolved by the leaching solutions used (Stewart et al., 2015) and may not have been sufficiently abundant to identify by XRD. Exchangeable radium was mobilized from sediments by ammonium acetate at the point of discharge of CWT-A (7%) and the downstream section B (9%) (Fig. 7). Stewart et al. (2015) reported that the ammonium acetate extraction step consistently mobilized the majority of barium in the samples of Marcellus Shale and associated rocks they investigated (implying substantial amounts in labile ion-exchange). In our study, radium also was mobilized (1) from "carbonate" phases by acetic acid, which accounted for 12% upstream, 4% at CWT-A discharge, and 8% for section B and (2) from "acid-soluble" phases dissolved by 0.1 M HCl, which accounted for 21% of radium in section B



K. Van Sice et al.

Fig. 7. The top panel depicts the radium activity in sediment samples following sequential extraction steps. The bottom panel depicts the XRD results of the samples. All samples were collected in 2016 unless otherwise noted.

compared to 2% upstream and 4% at CWT-A discharge. Stewart et al. (2015) reported the acetic-acid extraction step consistently removed the majority of manganese, the acetic acid and HCl steps removed the majority of iron, and the HCl step removed the majority of aluminum. Metals mobilized from sediments collected from the point of discharge, downstream, and upstream were consistent with the Stewart et al. (2015) results (Table S7).

The sequential extractions indicate that radium in the downstream sediments could occur as readily exchangeable ions on surfaces and in interlayer sites of clays, HMO, and HFO. Acidic pH (common with large rain events and spring snowmelts) could promote the release of radium and other cations from exchange sites, but not from more recalcitrant barite. These results are consistent with Landa and Reid (1983) and suggest that the radium downstream of CWTs is more abundant and more labile than radium in upstream sediments.

To examine the possibility of radium adsorption to stream sediments following disposal to surface water, we conducted adsorption experiments with a conventional O&G brine collected from the Appalachian Basin Oriskany Formation (see Supplemental Information). After exposure to different dilutions of conventional O&G wastewater, the radium activities in upstream sediments from CWT-A and CWT-E increased by 52–64% for $5\times$ dilutions, 22% for $25\times$ dilutions, and no detectable increase for $50\times$ dilutions (Fig. 8). The sorption and sequential extraction experiments indicate that some of the radium from O&G wastewater is sorbing to sediments or precipitating into mineral phase(s) that are capable of leaching radium under selected geochemical conditions.

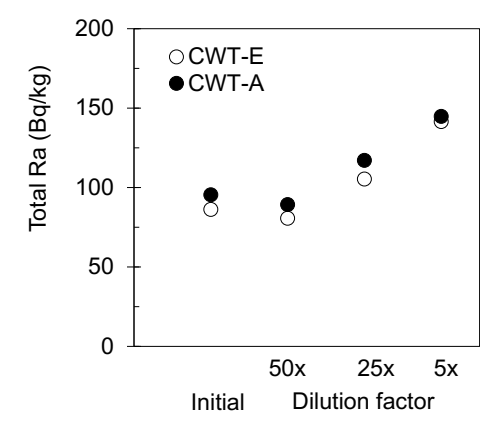


Fig. 8. Total radium activities of upstream sediments (i.e., background stream sediments) exposed to a conventional brine produced from the Oriskany Formation. Sediment samples were collected upstream of CWT A and CWT E and contained the same initial radium activity prior to exposure to the brine, which was diluted with distilled water at a range of dilution factors to mimic disposal to surface water and mixing.

3.5. Geochemical Modeling

The PHREEQC simulations of potential reactions after mixing the CWT-A effluent in various proportions with stream water of Blacklick Creek indicate aqueous radium could feasibly be attenuated within the stream by dilution, co-precipitation with a predominantly barite solid solution, and adsorption by HFO and HMO (Fig. 9, additional details in S9 and S10). The models for conservative mixing (Fig. 9a-b) indicate that all the mixtures have near-neutral to alkaline pH with a saturation index (SI) for barite or (Ba,Ra)SO₄ solid solution that is greater than or equal to 0 (indicating potential for precipitation). Celestite has a SI greater than or equal to 0 for the mixtures containing 95% or less upstream water. Thus, co-precipitation of radium with barite (and baritecelestite) solid solutions is indicated as a feasible mechanism of radium sequestration under conditions without sorbent, or with a moderate mass of sorbent per liter of solution (1000 mg/L HFO and 100 mg/L HMO) (Fig. 9c-d). Sediments in the upper 50-cm of core samples from Conemaugh River Lake have manganese and iron concentrations on the order of 1-10 percent, with Fe:Mn ratios as high as 10:1 (Burgos et al., 2017).

The mixing models (Fig. 9) and the companion adsorption models (Figs. 10, S11, and S12) indicate that co-precipitation and adsorption processes can operate simultaneously in the environment (Kondash et al., 2014), which combined may increase the total amount of radium sequestered. Without sorbent present, precipitation of (Ba,Ra)SO₄ is indicated to remove more than 85% of barium and 75% of radium from all the mixtures (Figs. S9 and S10). In contrast, where HFO and HMO coat fine sediment surfaces in contact with the water, adsorption of radium by HFO and HMO may account for substantial attenuation, particularly from more dilute waters that cancan occur during highstreamflow conditions or with increased distance downstream from the radium source. The models demonstrate that adsorption of barium and strontium can add to the removal of these ions, but also can lead to undersaturation of the aqueous solution with respect to barite, celestite, and associated solid solutions. In that case, adsorption becomes the dominant radium sequestration process (Figs. 9 and 10).

Generally, adsorption of the alkaline-earth cations by HMO is effective at acidic to neutral pH, whereas that by HFO becomes effective at near-neutral to alkaline pH (Fig. 10 and S11 and S12). For the modeled sorbent mass ratio of 1000:100 HFO:HMO and mixing ratio of 1:99 CWT-A:streamwater (representing high-streamflow or far downstream conditions), adsorption by HMO is indicated to remove as much as 40% of radium, 95% of barium, and 75% of strontium relative to the total concentrations in the initial mixture at near-neutral pH (Fig. 10b).

K. Van Sice et al. Applied Geochemistry 98 (2018) 393–403

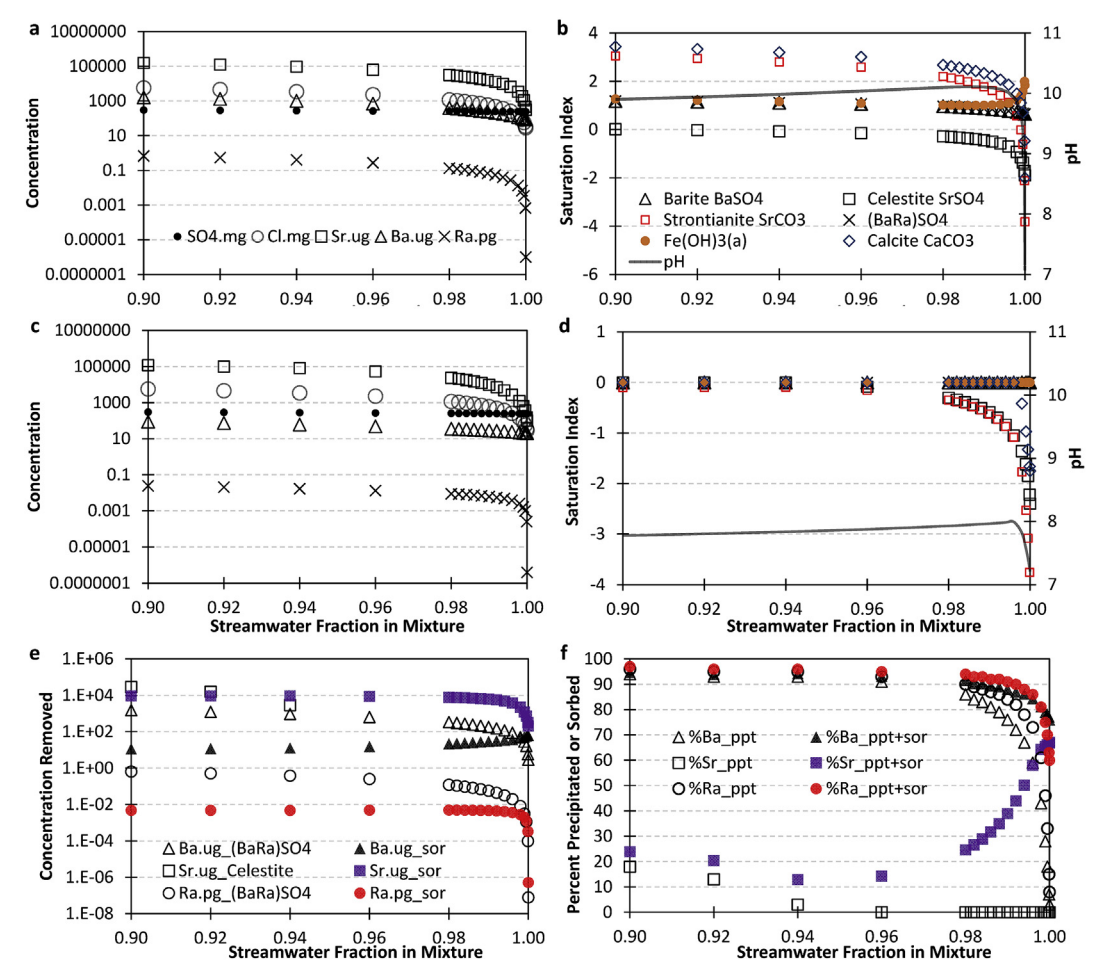


Fig. 9. PHREEQC simulation of the mixing of CWT-A effluent with Blacklick Creek streamwater: (a–b) conservative mixture without mineral precipitation or adsorption; and (c–f) equilibrium precipitation of pure phases and (Ba,Ra)SO₄ solid solution and adsorption by 1000 mg/L hydrous ferric oxide (HFO) and 100 mg/L hydrous manganese oxide (HMO). Variable concentration units are displayed for sulfate (SO₄, mg/L), chloride (Cl, mg/L), strontium (Sr, μ g/L), barium (Ba, μ g/L), and radium (Ra, μ g/L). (e) Aqueous concentrations of barium (Ba, μ g/L), strontium (Sr, μ g/L), and radium (Ra, μ g/L) removed from mixture by precipitation or adsorption and (f) corresponding percentage removed compared to conservative mixture. The fraction sorbed is indicated by difference between open and closed symbols for a given mixture. Minerals specified to precipitate upon reaching saturation include calcite (CaCO₃), dolomite (CaMg(CO₃)₂), gypsum (CaSO₄:2H₂O), amorphous ferric hydroxide (Fe(OH)₃, "HFO"), manganite (MnOOH; "HMO"), amorphous aluminum hydroxide (Al(OH)₃), barite (BaSO₄), witherite (BaCO₃), celestite (SrSO₄), and strontianite (SrCO₃). Note that the fraction of CWT-A in the mixture is difference between the streamwater fraction and 1.0; the streamwater fraction generally increases downstream of the point of discharge at CWT-A.

Decreasing HMO decreases the fraction adsorbed while increasing that precipitated as $(Ba,Ra)SO_4$ at the same pH (Figs. 10c,d, S12, and S13). With increased fractions of CWT-A effluent indicated by a mixing ratio of 10:90 (representing low-streamflow conditions or close to the effluent source), the concentrations of aqueous Sr, Ba, and Ra increase, leading to greater potential for their precipitation as sulfate compounds in addition to their attenuation by adsorption (Figs. 10a,c, S12, and S13).

Despite the superior capacity of HMO to adsorb Ra and Ba relative to HFO and its potential ability to decrease Ba concentrations to levels below saturation with respect to sulfate compounds, HMO can dissolve readily at about pH 4.5, where HFO and sulfate minerals could remain. Such acidic pH conditions and decreased ion concentrations can develop intermittently during high-flow events (episodic acidification, spring snowmelt). Strongly acidic or reducing conditions, which can develop in buried sediments, can mobilize sorbed ions through desorption, (competition with H⁺ or dissolving Mn^{+2,+3,+4} or Fe^{+2,+3} ions) or reductive dissolution of HFO and HMO. Where organic matter in sediments is the driving reductant, reduction at near-neutral pH generally would proceed in the sequence of HMO, HFO, and, finally, sulfate compounds (Appelo and Postma, 2005). Under extremely reducing conditions, halophilic anaerobes can mobilize the radium and

associated cations from sulfate compounds (Ouyang et al., 2017).

Although carbonate minerals were not detected in sediment samples by XRD, presumably because of low abundance, the sequential extractions indicated some radium was mobilized from carbonate phases by acetic acid (Fig. 5). The EDS images (Figs. S2- S8) indicated an association among Ba-Sr-S for some particles, additional Sr in other particles (not associated with Ba or S), and, in some samples, Ba-S associations were indicated where Sr was not detected. Strontianite (SrCO₃), calcite (CaCO₃), and aragonite (CaCO₃) were indicated to be supersaturated for the conservative mixtures containing as little as 0.1% CWT-A (Fig. 9b). Thus, precipitation of radium with aragonite, calcite, and/or strontianite solid solutions could be another mechanism for attenuation of radium (Langmuir and Riese, 1985). Nevertheless, with increasing dilution of the CWT effluent by streamwater, the potential to precipitate sulfate and carbonate minerals diminishes, and adsorption of Ra +2 and other cations by HMO and HFO becomes more important (Figs. 9 and 10). Widespread coal-mining activity in the Appalachian Plateau is a common source of aqueous iron and manganese, which oxidize and precipitate as HFO and HMO, forming ubiquitous coatings on streambed sediments (Cravotta, 2008); natural weathering processes in other environments also form HFO and HMO.

Despite their apparent ability to realistically simulate

Applied Geochemistry 98 (2018) 393-403

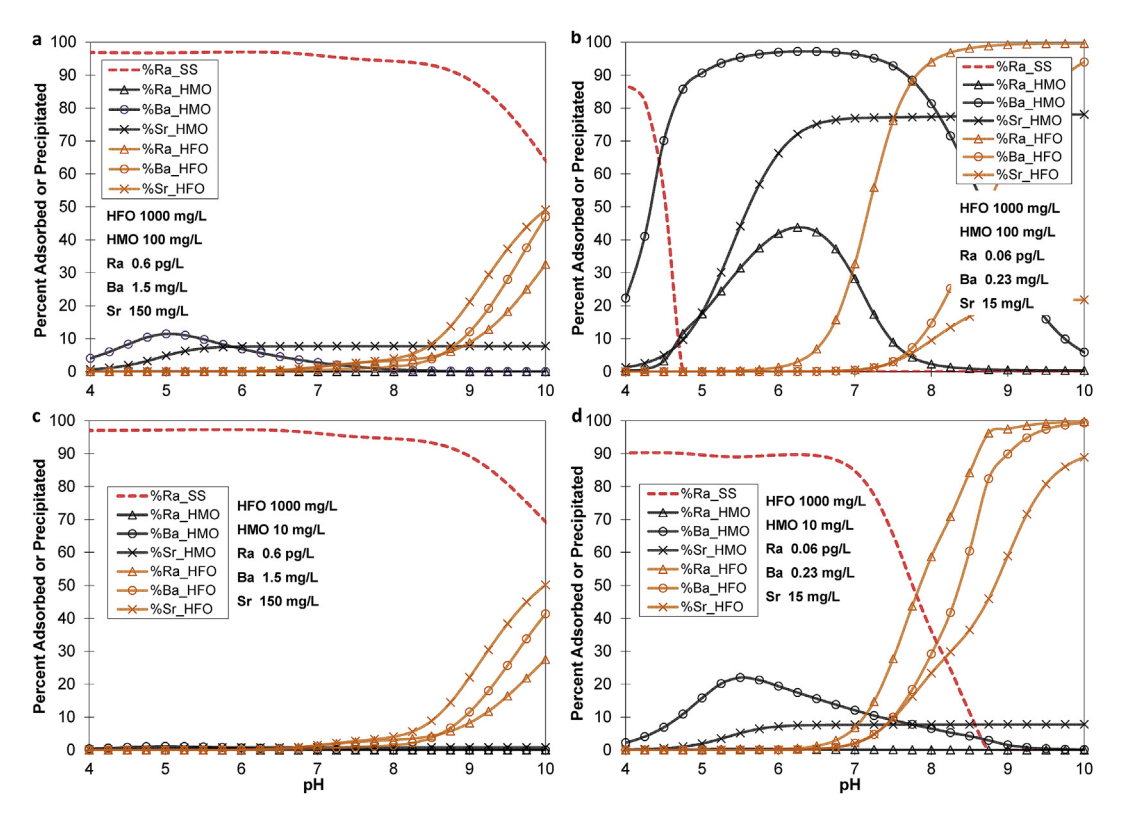


Fig. 10. Effects of pH, solute concentrations, and sorbent mass and composition (HFO, HMO) on attenuation of radium, barium, and strontium. Results of PHREEQC simulations are indicated for (a, c) 10:90 mixture of CWT-A effluent with streamwater or (b, d) 1:99 mixture in contact with (a, b) 1000 mg/L HFO and 100 mg/L HMO, or (c, d) 1000 mg/L HFO and 10 mg/L HMO. The percentage of radium removed as the solid solution, (Ba,Ra)SO₄ (%Ra_SS), is shown for comparison with that adsorbed by HFO and HMO. Note that adsorption of barium can decrease the amount of (Ba,Ra)SO₄ precipitated.

environmental processes that can attenuate aqueous radium in a stream system, the geochemical equilibrium models presented herein have limitations. For example, the models consider an ideal binary (Ba,Ra) SO₄ solid solution and only consider two types of sorbents. In fact, Ra may precipitate with more complex ternary solid solutions, such as (Ba,Sr,Ra)SO₄, over a wide range of temperatures (Vinograd et al., 2018a, 2018b). Such ternary phases can be modeled as non-ideal phases using PHREEQC (Rodríguez-Galán and Prieto, 2018); however, our understanding of the precise compositions of the Ra-bearing phases in our study is limited. We used a simplified representation of the (Ba,Ra) SO₄ solid solution based on other reports. Specifically, Vinograd et al. (2018a) reported a small quantity of RaSO₄ added to a Sr-rich solid solution results in nucleation of the binary (Ba,Ra)SO₄ solid solution. Furthermore, Zhang et al. (2014) reported that the removal of radium by interaction with barite or (Sr,Ba)SO₄ were similar, and Rosenberg et al. (2018) reported the removal of radium during seawater evaporation could be modeled adequately by precipitation of a binary solid solution of RaxBa1-xSO4. Our models also considered the potential for adsorption of radium, barium, and strontium by HFO and HMO, for which binding constants were available. We did not attempt to evaluate potential for adsorption by organic matter or various silicates. Because adsorption is sensitive to the mass and type of sorbent plus the ion composition, pH, and redox state of the solution, which affect HFO and HMO stability, the role of adsorption in the sequestration and release of radium is more difficult to predict and more variable than that of sulfate mineral precipitation. Lastly, our models assumed instantaneous reaction to equilibrium with respect to the specified mineral and solidsolution phases. Kinetic factors may need to be considered for accurate portrayal of dynamic systems. Regardless of such limitations, the empirical evidence from sequential extractions and brine-exposure experiments with radium-bearing sediments combined with geochemical modeling demonstrate the potential importance of both co-precipitation and adsorption processes for radium removal from the aqueous phase. Sequestration of radium into sediment is favored at the typical wastewater:streamwater ratios, but an increase of radium in the sediments is thus also an outcome.

3.6. Implications

Despite the policy change in 2011 that reduced disposal of unconventional wastes (i.e., Marcellus) to surface water in Pennsylvania, the continued disposal of conventional O&G wastewater has led to elevated radium activities in sediments at the point of discharge (Lauer et al., 2018). Elevated radium activities were observed in sediments at multiple facilities at similar or higher activities than those observed in previous studies (USEPA, 2011; Warner et al., 2013; Burgos et al., 2017). At a single facility (CWT-A) where we studied the distribution of radium in sediments over a 58 km transect, we observed a statistically significant increase in radium activities ($\sim 1.5 \times$ background) up to 31 km downstream of the discharge point, indicating greater range of the spatial distribution of elevated radium in the sediments than previously observed (Warner et al., 2013). Importantly, while remediation at this same facility (CWT-A) in 2015 led to lower activities in sediments at the point of discharge, the reduction was temporary, and activities are again elevated (10-20 × background) at the point of discharge in 2017. In addition, Ra concentrations may also continue to

Our observations of both mineralogy in the sediments and modeling of dilution of CWT-A effluent combined with model geochemical reactions (co-precipitation, adsorption) confirm that radium likely co-precipitates with barite and barite-celestite as the treated effluent enters the stream and accumulates in the sediment there, leading to the observed elevated activities. Adsorption of "exchangeable" radium is also indicated to be an important mode of occurrence in downstream sediments, particularly where fine-grained sediment and associated sorbents (HFO and HMO) are available, the concentrations of sulfate

and other solutes are diluted, and pH is near-neutral.

In conclusion, disposal of both conventional and unconventional O&G wastewater at multiple facilities to streams in Pennsylvania leads to accumulation of elevated radium activities in sediments. Transport of the sediment-bound radium, primarily as recalcitrant barite and baritecelestite solid solutions and secondarily as a surface-exchangeable cation, is apparent many kilometers downstream from the wastewater source. The radium co-precipitated with sulfate minerals or sequestered by adsorption generally is not bioavailable, but could be remobilized to more bioavailable aqueous species under reducing or acidic conditions, with the adsorbed fraction more likely to be released with minor changes to pH or oxidation-reduction potential. Thus, the radium accumulated in stream sediments at and downstream of O&G wastewater discharges implies the possibility of persistent environmental and human health concerns.

Acknowledgements

Partial funding for student support was provided by NSF:AIR-TT 1640634 and sediment sampling and processing NSF CBET:1703412. Use of manufacturers and trade names are for identification purposes only and do not constitute endorsement by the U.S. Geological Survey. We gratefully acknowledge two anonymous reviewers as well as Zoltan Szabo whose comments greatly improved the manuscript.

Appendix A. Supplementary data

Supplementary data to this article can be found online at https://doi.org/10.1016/j.apgeochem.2018.10.011.

References

- Akob, D.M., Cozzarelli, I.M., Dunlap, D.S., Rowan, E.L., Lorah, M.M., 2015. Organic and inorganic composition and microbiology of produced waters from Pennsylvania shale gas wells. Appl. Geochem. 60, 116–125.
- Akob, D.M., Mumford, A., Orem, W.H., Engle, M.A., Klinges, J.G., Kent, D.B., Cozzarelli, I.M., 2016. Wastewater disposal from unconventional oil and gas development degrades stream quality at a West Virginia injection facility. Environ. Sci. Technol. 50 (11), 5517–5525.
- Ames, L.L., McGarrah, J.E., Walker, B.A., Salter, F., 1983a. Uranium and radium sorption on amorphous ferric oxyhydroxide. Chem. Geol. 40, 135–148.
- Ames, L.L., McGarrah, J.E., Walker, B.A., 1983b. Sorption of trace constituents from aqueous solutions onto secondary minerals. II. Radium. Clay Clay Miner 31, 335–342. Appelo, C.A.J., Postma, D., 2005. Geochemistry, Groundwater and Pollution, 2nd. A.A. Balkema Publishers, Amsterdam, pp. 649.
- Ball, J.W., Nordstrom, D.K., 1991. User's manual for WATEQ4F, with revised thermodynamic data base and test cases for calculating speciation of major, trace, and redox elements in natural waters. U.S. Geol. Survey Open-File Rep. 91–183, 189.
- Beneš, P., Borovec, Z., Strejc, P., 1986. Interaction of radium with freshwater sediments and their mineral components: III. Muscovite and feldspar. J. Radioanal. Nucl. Chem. 98 (1), 91–103.
- Beneš, P., Strejc, P., Lukavec, Z., 1984. Interaction of radium with freshwater sediments and their mineral components. I. Ferric hydroxide and quartz. J. Radioanal. Nucl. Chem. 82 (2), 275–285.
- Beneš, P., Strejc, P., Lukavec, Z., 1985. Interaction of radium with freshwater sediments and their mineral components. II. Kaolinite and Montmorillonite. J. Radioanal. Nucl. Chem. 89 (2), 339–351.
- Blondes, M.S., Gans, K.D., Engle, M.A., Kharaka, Y.K., Reidy, M.E., Saraswathula, Varun, Thordsen, J.J., Rowan, E.L., Morrissey, E.A., 2017. U.S. Geological survey national produced waters geochemical database v2.3 (PROVISIONAL). https://energy.usgs.gov/EnvironmentalAspects/EnvironmentalAspectsofEnergyProductionandUse/ProducedWaters.aspx#3822349-data.
- Brantley, S.L., Yoxtheimer, D., Arjmand, S., Grieve, P., Vidic, R., Pollak, J., Llewellyn, G.T., Abad, J., Simon, C., 2014. Water resource impacts during unconventional shale gas development: the Pennsylvania experience. Int. J. Coal Geol. 126, 140–156.
- Burgos, W.D., Castillo-Meza, L., Tasker, T.L., Geeza, T.J., Drohan, P.J., Liu, X., Landis, J.D., Blotevogel, J., McLaughlin, M., Borch, T., Warner, N.R., 2017. Watershed-scale impacts from surface water disposal of oil and gas wastewater in western Pennsylvania. Environ. Sci. Technol. 51 (15), 8851–8860.
- Centeno, L.M., Faure, G., Lee, G., Talnagi, J., et al. Fractionation of chemical elements including REEs and ²²⁶Ra in stream contaminated with coal-mine effluent. Appl. Geochem. 19, p. 1085-1095.
- Chapman, M.J., Cravotta III, C.A., Szabo, Zoltan, Lindsey, B.D., 2013. Naturally occurring contaminants in the piedmont and blue ridge crystalline-rock aquifers and piedmont early mesozoic-rock aquifers, eastern United States. In: U.S. Geol. Survey Sci. Invest. Rep. 2013-5072, pp. 74.

- Cozzarelli, I.M., Skalak, K.J., Kent, D.B., Harper, D., Nagel, S.C., Iwanowicz, L.R., Orem, W.H., Akob, D.M., Jaeschke, J.B., Galloway, J., Kohler, M., Stoliker, D.L., Jolly, G.D., 2017. Environmental signatures and effects of an oil and gas wastewater spill in the Williston Basin, North Dakota. Sci. Total Environ. 579, 1781–1793.
- Cravotta, C.A., 2008. Dissolved metals and associated constituents in abandoned coalmine discharges, Pennsylvania, USA. Part 2: geochemical controls on constituent concentrations. Appl. Geochem. 23 (2), 203–226.
- Crespo, M., Gascon, J., Acena, M., 1993. Techniques and analytical methods in the determination of uranium, thorium, plutonium, americium and radium by adsorption on manganese dioxide. Sci. Total Environ. 130, 383–391.
- Dresel, P.E., Rose, A.W., 2010. Chemistry and Origin of Oil and Gas Well Brines in Western Pennsylvania: Pennsylvania Geological Survey, 4th Ser. Open-file Report OFOG 10–01.0.
- Dzombak, D.A., Morel, F.M.M., 1990. Surface Complexation Modeling: Hydrous Ferric Oxide. Wiley Interscience, pp. 393.
- Ferrar, K.J., Michanowicz, D.R., Christen, C.L., Mulcahy, N., Malone, S.L., Sharma, R.K., 2013. Assessment of effluent contaminants from three facilities discharging Marcellus shale wastewater to surface waters in Pennsylvania. Environ. Sci. Technol. 47 (7), 3477–3481
- Giffaut, E., Grivé, M., Blanc, P., Vieillard, P., Colàs, E., Gailhanou, H., Gaboreau, S., Marty, N., Madé, B., Duro, L., 2014. Andra thermodynamic database for performance assessment: Thermo Chimie. Appl. Geochem. 49, 225–236.
- Good, K.D., VanBriesen, J.M., 2016. Current and potential future bromide loads from coal-fired power plants in the Allegheny River basin and their effects on downstream concentrations. Environ. Sci. Technol. 50 (17), 9078–9088.
- Gregory, K.B., Vidic, R.D., Dzombak, D.A., 2011. Water management challenges associated with the production of shale gas by hydraulic fracturing. Elements 7 (3), 181–186.
- Haluszczak, L.O., Rose, A.W., Kump, L.R., 2013. Geochemical evaluation of flowback brine from Marcellus gas wells in Pennsylvania, USA. Appl. Geochem. 28 (0), 55–61.
- Harkness, J., Dwyer, G.S., Warner, N.R., Parker, K.M., Mitch, W.A., 2015. Iodide, bro-mide, and ammonium in hydraulic fracturing and oil and gas wastewaters: environmental implications. Environ. Sci. Technol. 49 (3), 1955–1963.
- Hladik, M.L., Focazio, M.J., Engle, M., 2014. Discharges of produced waters from oil and gas extraction via wastewater treatment plants are sources of disinfection by-products to receiving streams. Sci. Total Environ. 466, 1085–1093.
- International Atomic Energy Agency, 2014. The Environmental Behaviour of Radium: Revised Edition. International Atomic Energy Agency Technical Reports Series No. 476, Vienna, Austria.
- Kargbo, D.M., Wilhelm, R.G., Campbell, D.J., 2010. Natural gas plays in the Marcellus shale: challenges and potential opportunities. Environ. Sci. Technol. 44 (15), 5679–5684.
- Kondash, A.J., Warner, N.R., Lahav, Ori, Vengosh, Avner, 2014. Radium and barium removal through blending hydraulic fracturing fluids with acid mine drainage. Environ. Sci. Technol. 48 (2), 1334–1342.
- Landa, E.R., Reid, D.F., 1983. Sorption of radium-226 from oil-production brine by sediments and soils. Environ. Geol. 5 (1), 1–8.
- Langmuir, D., Riese, A.C., 1985. The thermodynamic properties of radium. Geochem. Cosmochim. Acta 49, 1593–1601.
- Lauer, N.E., Hower, J.C., Hsu-Kim, H., Taggart, R.K., Vengosh, A., 2015. Naturally occurring radioactive materials in coals and coal combustion residuals in the United States. Environ. Sci. Technol. 49 (18), 11227–11233.
- Lauer, N.E., Warner, N.R., Vengosh, A., 2018. Sources of radium accumulation in stream sediments near disposal sites in Pennsylvania: implications for disposal of conventional oil and gas wastewater. Environ. Sci. Technol. 52 (3), 955–962.
- Menzie, C.A., Southworth, B., Stephenson, G., Feisthauer, N., 2008. The importance of understanding the chemical form of a metal in the environment: the case of barium sulfate (barite). Human Ecol. Risk Assess. 14 (5), 974–991.
- NYDEC, 1999. An Investigation of Naturally Occurring Radioactive Materials (NORM) in Oil and Gas Wells in New York State, Albany, New York.
- Osborn, S.G., McIntosh, J.C., 2010. Chemical and isotopic tracers of the contribution of microbial gas in Devonian organic-rich shales and reservoir sandstones, northern Appalachian Basin. Appl. Geochem. 25 (3), 456–471.
- Ouyang, B., Akob, D.M., Dunlap, D., Renock, D., 2017. Microbially mediated barite dissolution in anoxic brines. Appl. Geochem. 76, 51–59.
- PADEP, 2016a. PA DEP Oil and Gas Reporting Website: Statewide Data Downloads by Reporting Period. Pennsylvania Department of Environmental Protection, Harrisburg, PA.
- PADEP, 2016b. Technologically Enhanced Naturally Occurring Radioactive Materials (TENORM) Study Report. Pennsylvania Department of Environmental Protection, Harrisburg, PA.
- Parekh, P., Haines, D., Bari, A., Torres, M., 2003. Non-destructive determination of ²²⁴Ra, ²²⁶Ra and ²²⁸Ra concentrations in drinking water by gamma spectroscopy. Health Phys. 85 (5), 613–620.
- Parkhurst, D.L., Appelo, C.A.J., 2013. Description of input and examples for PHREEQC version 3—a computer program for speciation, batch-reaction, one-dimensional transport, and inverse geochemical calculations. USGS Tech. Meth. 6-A43, 497.
- Pourret, O., Davranche, M., 2013. Rare earth element sorption onto hydrous manganese oxide: a modeling study. J. Colloid Interface Sci. 395, 18–23.
- Rodríguez-Galán, R.M., Prieto, M., 2018. Interaction of nonideal, multicomponent solid solutions with water: a simple algorithm to estimate final equilibrium states. Geochem. Geophys. Geosystems. 19, 1348–1359.
- Rosenberg, Y.O., Sade, Z., Ganor, J., 2018. The precipitation of gypsum, celestine, and barite and coprecipitation of radium during seawater evaporation. Geochem. Cosmochim. Acta 233, 50–65.
- Rowan, E., Engle, M., Kirby, C., Kraemer, T., 2011. Radium Content of Oil- and Gas-field

- Produced Waters in the Northern Appalachian Basin (USA)—Summary and Discussion of Data: U.S. Geological Survey Scientific Investigations Report 2011–5135. U.S. Geological Survey.
- Rowan, E.L., Engle, M.A., Kraemer, T.F., Schroeder, K.T., Hammack, R.W., Doughten, M.W., 2015. Geochemical and isotopic evolution of water produced from Middle Devonian Marcellus shale gas wells, Appalachian basin, Pennsylvania. AAPG (Am. Assoc. Pet. Geol.) Bull. 99 (2), 181–206.
- Sajih, M., Bryan, N., Livens, F., Vaughan, D., Descostes, M., Phrommavanh, V., Nos, J., Morris, K., 2014. Adsorption of radium and barium on goethite and ferrihydrite: a kinetic and surface complexation modelling study. Geochem. Cosmochim. Acta 146, 150–163.
- Skalak, K.J., Engle, M.A., Rowan, E.L., Jolly, G.D., Conko, K.M., Benthem, A.J., Kraemer, T.F., 2014. Surface disposal of produced waters in western and southwestern Pennsylvania: potential for accumulation of alkali-earth elements in sediments. Int. J. Coal Geol. 126, 162–170.
- Stewart, B.W., Chapman, E.C., Capo, R.C., Johnson, J.D., Graney, J.R., Kirby, C.S., Schroeder, K.T., 2015. Origin of brines, salts and carbonate from shales of the Marcellus Formation: evidence from geochemical and Sr isotope study of sequentially extracted fluids. Appl. Geochem. 60, 78–88.
- Szabo, Z., dePaul, V.T., Fischer, J.M., Kraemer, T.F., Jacobsen, E., 2012. Occurrence and geochemistry of Radium in aquifers used for drinking water in the United States. Appl. Geochem. 27, 729–752.
- Tasker, T.L., Piotrowski, P.K., Dorman, F.L., Burgos, W.D., 2016. Metal associations in Marcellus shale and fate of synthetic hydraulic fracturing fluids reacted at high pressure and temperature. Environ. Eng. Sci. 33 (10), 753–765.
- Tonkin, J.W., Balistrieri, L.S., Murray, J.W., 2004. Modeling sorption of divalent metal cations on hydrous manganese oxide using the diffuse double layer model. Appl. Geochem. 19 (1), 29–53.

- USEPA, 2000. National Primary Drinking Water Regulations; Radionuclides: Final Rule. USEPA, Washington, D.C.
- USEPA, 2011. Voluntary sampling data from oil and gas wastewater treatment facilities. available at. http://www.epa.gov/region3/marcellus_shale/#epawpadep.
- Vengosh, A., Hirschfeld, D., Vinson, D., Dwyer, G., Raanan, H., Rimawi, O., Al-Zouri, A., Akkawi, E., Marie, A., Haquin, G., Zaarur, S., Ganor, J., 2009. High naturally occurring radioactivity in fossil groundwater from the Middle East. Environ. Sci. Technol. 43, 1769–1775.
- Vengosh, A., Jackson, R.B., Warner, N.R., Darrah, T.H., Kondash, A.J., 2014. A critical review of the risks to water resources from unconventional shale gas development and hydraulic fracturing in the United States. Environ. Sci. Technol. 48, 8334–8348.
- Vinograd, V.L., Kulik, D.A., Brandt, F., Klinkenberg, M., Weber, J., Winkler, B., Bosbach, D., 2018a. Thermodynamics of the solid solution aqueous solution system (Ba,Sr,Ra) $SO_4 + H_2O$: I. The effect of strontium content on radium uptake by barite. Appl. Geochem. 89, 59–74.
- Vinograd, V.L., Kulik, D.A., Brandt, F., Klinkenberg, M., Weber, J., Winkler, B., Bosbach, D., 2018b. Thermodynamics of the solid solution aqueous solution system (Ba,Sr,Ra) SO₄ + H₂O: II. Radium retention in barite-type minerals at elevated temperatures. Appl. Geochem. 93, 190–208.
- Warner, N.R., Christie, C.A., Jackson, R.B., Vengosh, A., 2013. Impacts of shale gas wastewater disposal on water quality in western Pennsylvania. Environ. Sci. Technol. 47 (20), 11849–11857.
- Wilson, J.M., VanBriesen, J.M., 2012. Oil and gas produced water management effects on surface drinking water sources in Pennsylvania. Environ. Pract. 14 (1), 1–13.
- Zhang, T., Gregory, K., Hammack, R.W., Vidic, R.D., 2014. Co-precipitation of radium with barium and strontium sulfate and its impact on the fate of radium during treatment of produced water from unconventional gas extraction. Environ. Sci. Technol. 48 (8), 4596–4600.